Investigation of the Surface Chemical Structure of Some Biomedical Poly(amidoamine)s Using High-Resolution X-ray Photoelectron Spectroscopy and Time-of-Flight Secondary Ion Mass Spectrometry

A. G. Shard,[†] L. Sartore,[‡] M. C. Davies,*[,†] P. Ferruti,[‡] A. J. Paul,[§] and G. Beamson[||]

Laboratory of Biophysics and Surface Analysis, Department of Pharmaceutical Sciences, The University of Nottingham, Nottingham NG7 2RD, U.K., Dipartimento di Chimica e Fisica per i Materiali, Università di Bresica, Via Branze 38, 25123 Bresica, Italy, CSMA, Armstrong House, Oxford Road, Manchester M1 7ED, U.K., and RUSTI, DRAL Daresbury Laboratories, Warrington WA4 4AD, U.K.

Received February 21, 1995; Revised Manuscript Received September 5, 1995[⊗]

ABSTRACT: A series of poly(amidoamine) spin cast films have been analyzed by both high-resolution XPS and ToF-SIMS. The XPS results are in excellent agreement with those expected from the bulk polymeric structure. Differences between isomeric polymers were apparent in the valence band spectra. Also, the susceptibility to X-ray-induced degradation was noted and studied in some of the polymers with loss of carboxylic acid groups and quaternized nitrogen being the most notable features. High-mass resolution ToF-SIMS produced complex spectra often with numerous peaks of differing elemental composition appearing at the same nominal mass. All of the prominent signals are assigned to ions derived from simple fragmentations of each polymer. Species could be grouped easily into series of ions derived from specific portions of the polymers and important mechanistic processes deduced from the intensities of common species.

Introduction

Poly(amidoamine)s (PAAs) are regular teramino polymers obtained, in a linear form by stepwise polyaddition of primary monoamines or bis secondary amines to bisacrylamides:[1]

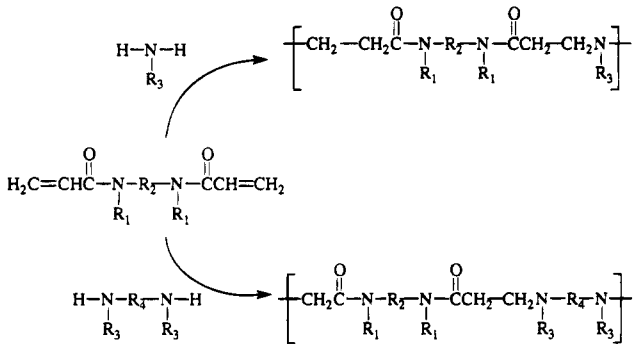

The polymerization reaction can be carried out in water and at room temperature without using any catalyst. It takes place easily with almost every aliphatic and cycloaliphatic amine, and also in the presence of side substituents containing functional groups such as hydroxyl, carboxylic acid, and additional tertiary amine. Most PAAs are water soluble or at least water swellable. In aqueous solution, they behave as bases of medium strength whose pK_a's (which, unlike what is usually encountered in the polyelectrolyte's domain, are "real" and not "apparent") are usually within the range of 7–9 (first ionization) or 4–7 (second ionization, when two basic nitrogens are present in the repeat unit).

PAAs are attracting interest within the biomedical community for a number of clinical applications either as biomaterials or for biomaterials modification. The main interest of PAAs in the medical field lies in the heparin-complexing ability of many of them, coupled with the absence of obvious interactions with normal blood components such as red blood cells, platelets, and plasma proteins. This was discovered as early as 1973,[2] and many papers have appeared on this subject since. Heparin complexation takes place either with soluble PAAs, some of which are able to neutralize the anticoagulant activity of heparin much in the same way as protamine sulfate does, or with cross-linked PAAs and insoluble PAA-based materials, which are able to absorb heparin stably from its aqueous solutions.

Heparin is added to the blood of patients to prevent thrombus formation during extracorporeal processes such as hemodialysis. The anticoagulant nature of heparin results in patients suffering from side effects, which include delayed thrombogenic responses and interference with lipid metabolism. It has been suggested therefore that the heparin used during hemodialysis should be removed prior to the reintroduction of blood into the patient, and there are high hopes of utilizing heparin-adsorbing resins in clinical practice as bioactive components of deheparinization filters for blood. These filters will be used for achieving regional heparinization of extracorporeal circuits in, for example, hemodialysis.[3,4] A method for avoiding systemic heparinization of the patient by confining heparin to the extracorporeal circuit would be of immense benefit to the many "at risk" patients undergoing routine dialysis treatments.

More recently, PAAs are being considered as soluble carriers for delivering anticancer drugs. To this purpose their hydrophilicity, degradability,[5] and the facility of further functionalization appear very appealing. A preliminary *in vitro* study[6] has demonstrated that some PAAs are endowed with fairly good cell compatibility. In other words, their cell toxicity, at least with the cell lines considered, is low, much lower, for instance, than that of poly(L-lysine), which is no longer considered as

[†] The University of Nottingham.
[‡] Università di Bresica.
[§] CSMA.
[||] RUSTI.
[⊗] Abstract published in *Advance ACS Abstracts,* November 1, 1995.

0024-9297/95/2228-8259$09.00/0

Table 1. Typical PAAs Selected for XPS and ToF-SIMS Studies

no.	monomers[a]	repeat structure	η_{sp}/C^b (dL/g)
1	BP–2MeP	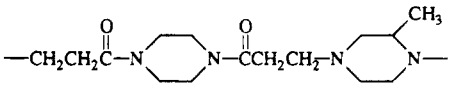	0.207
2	MBA–2MeP	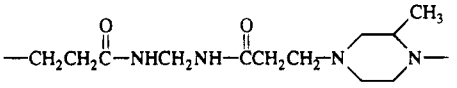	0.118
3	BAC–2MeP	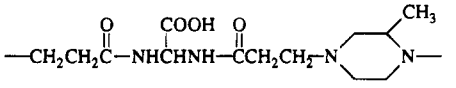	0.196
4	MBA–DMEDAsim	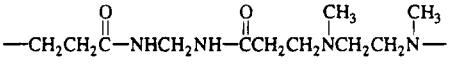	0.14
5	BAC–DMEDAsim	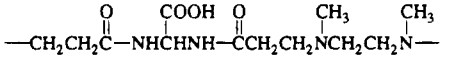	0.265
6	BAC–DMEXA	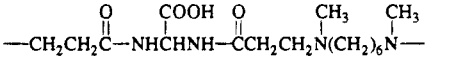	0.27
7	BAC–DMEDAasim	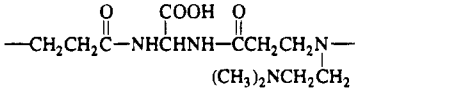	0.26

[a] Key: BP = 1,4-bisacryloylpiperazine, MBA = *N,N'*-methylenebisacrylamide, BAC = 2,2-bis(acrylamidoacetic acid), 2MeP = 2-methylpiperazine, DMEDAsim = *N,N'*-dimethylethylenediamine, DMEXA = *N,N'*-dimethylhexamethylenediamine, DMEDAasim = *N,N*-dimethylethylenediamine. [b] C = 0.2% in 0.1 M NaCl.

a potential cationic carrier precisely because of its high toxicity.

Because of the aqueous solubility of PAAs, for many of the potential applications it is necessary to either render them insoluble by cross-linking or graft them to a nonsoluble substrate. It is therefore important to have the capacity to determine whether any immobilization technique has been successful in producing a PAA-rich surface. For this purpose, surface analytical techniques such as X-ray photoelectron spectroscopy (XPS) and time-of-flight secondary ion mass spectrometry (ToF-SIMS) are appropriate techniques. Currently there are no published reports in which XPS or ToF-SIMS has been applied to PAAs, and we present here the first characterization of PAAs by both methods. These techniques have been employed previously to investigate the interfacial chemistry of a number of biomedical polymers including polyesters,[7,8] polyorthoesters,[8,9] and polyanhydrides.[8,10]

In addition to characterizing novel polymeric surfaces, these studies provide valuable information with regard to the XPS and ToF-SIMS techniques themselves and the manner in which polymers interact with energetic radiation.

Experimental Section

Polymer Synthesis and Characterization. (a) Instruments. Intrinsic viscosities were measured at 32 °C in 0.1 M NaCl by means of Ubbelohde viscometers. IR spectra were run on a Jasco 5300 FT-IR spectrophotometer, with films cast from water on ZnSe windows. Gel permeation chromatograms were obtained making use of TSK-GEL G 3000 PW and TSK-GEL G 4000 PW columns connected in series, with 0.1 M Tris buffer–0.2 M NaCl (pH 8) as the mobile phase, and a flow rate of 1 mL/min (Knauer model HPLC pump 64), while the samples were checked by a Knauer UV detector operating at 230 nm.

(b) Materials. All starting materials were reagent grade purchased from Fluka Co. (Buchs, Switzerland) and used without further purification. 1,4-Bis(acryloylpiperazine) (BP) and 2,2-bis(acrylamidoacetic acid) (BAC) were purchased from Aldrich Co. (Steinheim, West Germany) and recrystallized from methanol just before use in the presence of a small amount of 4-methoxyphenol as radical inhibitor.

(c) General Recipe for the Preparation of Linear Vinyl-Terminated PAAs. Bisacrylamide (1.15 mol) and 1 mol of a primary monoamine or secondary bisamine were thoroughly mixed in the presence of water (~2 mL/g of the sum of the monomers) or another hydroxylated solvent. If the bisacrylamide was BAC, an equimolar quantity of 2 M NaOH was used. Catalysts were not required, but a small amount of radical inhibitor was added in order to avoid radical polymerization of the acrylic monomer. It was better to run the reaction under nitrogen atmosphere to avoid discolorations, but this was not strictly necessary. The preferred reaction temperatures were between 20 and 50 °C. After waiting between 1 and 7 days according to the reaction temperature and the nature of the monomers (steric hindrance on the aminic nitrogen greatly affects the polymerization rate), the product can be isolated. The solution was ultrafiltered in an Amicon system with a YM 3 membrane. If the bisacrylamide was BAC, it was necessary to eliminate the sodium salt. To this purpose, the solution was brought to pH 3 with 1 M HCl and ultrafiltered with water until no chlorine was detected in the waste water. The product was finally lyophilized with a yield of 70%. The dry powder was further purified by continuous extraction with ether in order to minimize contamination with silicone oil, which is a common laboratory contaminant.

The FTIR and ^{1}H NMR spectra of the products were as expected from their structure.

For the XPS and SIMS studies, seven PAAs were selected, deriving from three bisacrylamides and four amines. Their structures are given in Table 1. These polymers were characterized in terms of molecular weight distribution by means of analytical GPC. To this purpose a calibration curve had been determined making use of PAA purposely prepared and analyzed by NMR techniques.[11] The results are summarized in Table 2.

Surface Analysis. (a) XPS Analysis. The XPS spectra were acquired using a Scienta ESCA300 electron spectrometer employing monochromated Al Kα (1486.7 eV) X-rays. This instrument has been described in detail elsewhere.[12,13] The X-ray gun was operated at 2.8 kW, and the electron take-off angle to the spectrometer was 90°. In all cases, the polymeric

Table 2. Molecular Weight and Molecular Weight Distributions of the Polymers

products	M_w	M_n	d
BP–2MeP	2850	1720	1.66
MBA–2MeP	2129	1401	1.52
BAC–2MeP	9538	6231	1.53
MBA–DMEDAsim	2649	1840	1.44
BAC–DMEDAsim	9663	6895	1.40
BAC–DMEXA	7753	5824	1.33
BAC–DMEDAasim	7790	5882	1.32

films were thin enough to obviate the need for charge compensation, yet thick enough that electrons from the silicon substrate could not be detected. Survey spectra (0–1150-eV binding energy) were obtained using a pass energy of 300 eV and a slit width of 1.9 mm. Narrow scans of elemental core lines were taken with a pass energy of 150 eV and slit widths of 0.5 mm. Valence band spectra (0–35-eV binding energy) and spectra following X-ray degradation (over 11 h) were acquired in a single experiment with a pass energy of 150 eV and a slit width of 1.9 eV. Collection and analysis of data was performed on the Scienta ESCA300 data system software. Peak fitting of the core level spectra was carried out using a standard methodology.[8]

Charge referencing experiments were carried out by spin casting a thin layer of paraffin wax (~0.5% solution in chloroform) either over the PAA film in the case of water-soluble polymers or from a mixed solution of wax and poly(amidoamine). Care was taken to ensure that the N 1s region was still visible in the XPS spectra. The N 1s binding energy positions were measured relative to the paraffin wax C 1s peak (at 285 eV), and these nitrogen positions were then used to calibrate the original spectra. This method was chosen instead of using an "internal" reference, such as using a hydrocarbon signal from the polymer itself, because in most of the polymers under study here the hydrocarbon peak is weak in intensity and therefore unreliable in position or nonexistent. Since no other common reference could be found for the PAAs, the paraffin wax method was deemed most suitable. It should be noted that there are a few potential problems with the use of paraffin wax, the main one being that the wax may not be miscible with PAA polymers and would thus form discrete domains throughout the sample. This could result in differential electrical charging between PAA and wax domains which would invalidate the charge referencing.

(b) SIMS Analysis. For all polymers, ToF-SIMS spectra were obtained using a VG IX23S instrument based on a Poschenrieder design and equipped with a 30-keV Ga^+ primary ion source operated with a pulse length duration of ~20 ns.[14] For each sample, both positive and negative secondary ion spectra were collected using a total primary ion dose which did not exceed 2×10^{11} ions cm^{-2}. Such a dose lies well below the damage threshold value of 1×10^{13} ions cm^{-2} for *static* SIMS.[15]

High-mass resolution positive ion spectra were also obtained for five of the polymers using a Physical Electronics PHI 7000 instrument comprising a grid design reflectron analyzer and a 8-keV Cs^+ primary ion source operated with a pulse length duration of ~1 ns.[16] For all samples analyzed, mass resolutions of $M/\Delta M > 7000$ at m/z 29 were achieved. Peak positions were determined using the fwhm centroid calculation.[16] This method was used for both the calibration of the spectra and the mass determination of the peaks. For each spectrum, an initial calibration using a three-peak extrapolation (C_xH_y at m/z 15, 27, and 41) was carried out. Further calibrations, using up to seven peaks were also carried out by incorporating additional peaks in the m/z range 50–120 into the calibration procedures. As detailed elsewhere,[16] the accuracy of the mass assignment for each peak was calculated according to the formula $[M_{measd} - M_{exact}]/M_{exact} \times 10^6$ ppm. The mass accuracies of most of the intense signals in each spectrum were <10 ppm, and the mass accuracies of all other relevant signals in each spectrum were <30 ppm, where the higher ppm values often corresponded to signals of lower intensity.[16] For each sample, the total primary ion dose did not exceed 5×10^{11} ions cm^{-2}.

(c) Sample Preparation. PAA solutions (~1% w/v) were spin cast onto either clean aluminum foil for SIMS or argon sputter cleaned silicon for XPS analyses. It was found that solutions of polymers BP–2MeP, MBA–2MeP, and MBA–DMEDAsim (i.e., those not containing carboxylic acid groups) in water did not dry evenly, and consequently these polymers were cast from analytical grade chloroform.

Table 3. Experimental and Theoretical Surface Atomic Concentrations of PAAs

	experimental (%)				theoretical (%)			
polymer	C	O	N	Cl	C	O	N	Cl
BP–2MeP	72.0	9.3	18.7	0.0	71.4	9.5	19.0	0.0
MBA–2MeP	68.0	12.0	20.0	0.0	66.7	11.1	22.2	0.0
BAC–2MeP	60.2	19.1	19.8	0.9	61.3	18.9	18.9	0.9
MBA–DMEDAsim	64.6	11.7	23.5	0.2	64.6	11.8	23.4	0.2
BAC–DMEDAsim	57.7	20.4	19.0	2.9	58.1	19.4	19.4	3.1
	58.6	18.8	19.4	3.2				
BAC–DMEXA	64.3	15.0	15.9	4.8	63.6	15.9	15.9	4.6
	64.0	15.8	15.8	4.5				
BAC–DMEDAasim	58.7	19.4	20.0	1.9	58.6	19.6	19.6	1.9
	58.1	20.1	20.0	1.8				

Table 4. C 1s Binding Energies Determined for PAA Functionalities

	Poly(amidoamine)					
polymer	*HC*	*CCON*	*CN*	*NCN*	*CON*	*COOH*
BP–2MeP	284.62	285.27	285.90		287.93	
MBA–2MeP	284.93	285.56	285.99	287.25	288.37	
BAC–2MeP	285.02	285.59	286.37	287.33	288.26	288.94
MBA–DMEDAsim		285.19	285.71	286.95	288.09	
BAC–DMEDAsim		285.47	286.49	287.26	288.25	288.93
BAC–DMEXA	285.17	285.62	286.48	287.36	288.24	289.01
BAC–DMEDAasim		285.32	286.28	287.14	288.09	288.80
average (PAA)	284.94	285.43	286.17	287.21	288.18	288.92
literature	285.00	285.40	285.97	287.50	288.11	289.26

Results and Discussion

To aid understanding, the XPS and ToF-SIMS analysis of the PAAs will be discussed separately.

XPS. (a) Core-Level Spectra. Survey spectra revealed the presence of three elements: carbon, oxygen, and nitrogen. Many of the polymers also contained a significant quantity of chlorine, the binding energy shift of which (~197.8 eV Cl $2p_{3/2}$) was typical of the chloride anion.[17] Polymer BAC–DMEXA also showed a small peak due to sodium (Na 1s ~1072 eV).[17] Atomic compositions for each polymer were calculated using the narrow-scan peak areas and the appropriate sensitivity factors for each element. Theoretical values are simply calculated from the number of each type of atom in the polymer repeat unit. Experimental and theoretical (taking into account the presence of chlorine) atomic compositions are given in Table 3. Where more than one acquisition was performed on a fresh polymer sample, in the case of those polymers which were degraded overnight, both sets of data are included in the table. There is an excellent agreement between experimental and theoretical data for each polymer, which indicates that the surfaces are contamination free, at least within the limits of the XPS technique.

The narrow scans of each polymer showed extensive structure in the C 1s region; examples are given in Figure 1a,b, with fitted peaks. Each of the peaks represents a specific carbon environment within the polymers. There are six readily definable groups, and these are listed in Table 4 along with the binding energies that we have found in this work and typical literature values for the same groups in different polymers.[8,18] It can be seen that in general there is good consistency between the different poly(amidoamine)s and the same functional groups found in other polymers. The validity of the charge referencing approach can be assessed by comparison of binding energies of various functional groups between polymers. The BP–2MeP

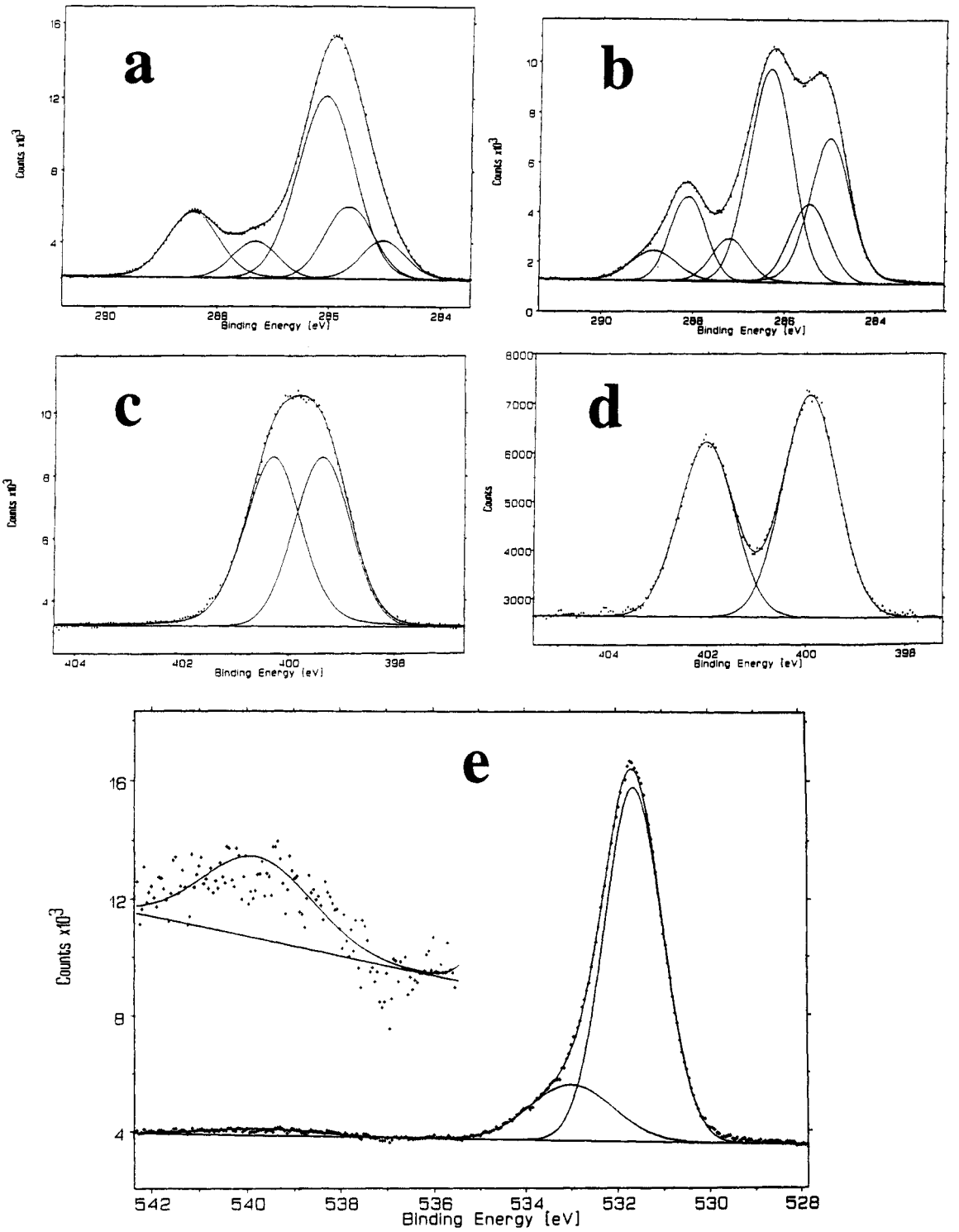

Figure 1. C 1s region of (a) MBA–2MeP and (b) BAC–DMEXA. N 1s region of (c) BP–2MeP and (d) BAC–DMEXA. (e) O 1s region of BAC–2MeP with expanded region showing shake-up feature.

polymer/paraffin wax mixture demonstrated a strong retention of chloroform (as evidenced by the appearance of a Cl 2p peak, Cl $2p_{3/2}$ = 201.20-eV binding energy) which did not occur with paraffin wax or BP–2MeP on their own. Chloroform retention under ultrahigh vacuum is not unknown and can actually be useful for determining polymer basicity,[19] but the interaction between polymer, wax, and solvent makes the charge referencing for this compound unreliable. Indeed, this polymer's C 1s binding energy values as determined by our charge referencing approach are ~0.3 eV lower than is normal for other PAAs. Polymers MBA–DMEDAsim and BAC–DMEDAasim also appear to have slightly lower binding energy values than other PAAs, and this may indicate that accurately charge referencing these polymers with paraffin wax is not possible. The remaining four compounds give binding energy values that are in good agreement with each other (±0.12 eV, with the exception of the *C*N groups), and the hydrocarbon functionalities appear close to 285 eV.

The *C*N group chemical shift varies more substantially than any other C 1s functionality between different poly(amidoamine)s (the extremes being 285.71 and 286.49 eV). Variability in this shift can be related not just to charge referencing problems but also to the amount of protonated amine found in the polymer. It is to be expected that carbon atoms bound to a positive charge center will demonstrate higher binding energies

Table 5. Experimental vs Theoretical Component Peak Areas for C 1s Spectra of PAAs

polymer		% contribution to C 1s area					
		CH	CCON	CN	NCN	CON	COOH
BP–2MeP	exp	6.7	13.1	66.8		13.4	
	theory	6.7	13.3	66.7		13.3	
MBA–2MeP	exp	8.6	17.0	49.8	7.9	16.7	
	theory	8.3	16.7	50.0	8.3	16.7	
BAC–2MeP	exp	8.5	14.9	45.6	7.7	14.8	8.5
	theory	7.7	15.4	46.2	7.7	15.4	7.7
MBA–DMEDAsim	exp		17.9	53.1	10.1	18.9	
	theory		18.2	54.5	9.1	18.2	
BAC–DMEDAsim	exp		17.3	49.0	8.8	16.6	8.3
	exp		17.0	49.1	8.6	16.6	8.7
	theory		16.7	50.0	8.3	16.7	8.3
BAC–DMEXA	exp	25.2	12.5	37.5	6.6	12.4	5.8
	exp	24.3	13.1	38.1	6.1	11.8	6.6
	theory	25.0	12.5	37.5	6.3	12.5	6.3
BAC–DMEDAasim	exp		17.5	49.5	8.6	16.0	8.4
	exp		16.8	49.9	8.8	16.7	7.8
	theory		16.7	50.0	8.3	16.7	8.3

than those attached to a neutral atom,[8] and this is found to be the case. The *C*OOH group chemical shifts are lower than the literature values by roughly 0.3 eV. It is thought that a substantial proportion of these groups (see later) exist as the anion, the presence of which will reduce the binding energy at which this carbon atom appears.

A comparison of the component peak areas expressed as a percentage of the total C 1s area to values calculated from the polymer stoichiometry is shown in Table 5. Good agreement is achieved between the observed and calculated values for functional group concentration. Variation between the peak fit areas and those expected are always within 1% of the total C 1s area. Although the sampling depth is quite large with a take-off angle of 90°, ~9 nm,[20] it appears from this result that the surfaces of all these polymers are free from organic contaminants and surface organization effects (caused by, for instance, rearrangements and residual monomeric species).

Most of the polymers contain more than one component in the N 1s region. Panels c and d of Figure 1 show the N 1s regions from polymers BP–2MeP nd BAC–DMEXA. BP–2MeP clearly shows two overlapping peaks of roughly equal intensity; these can be assigned to the amine and the amide nitrogen environments. None of the other polymers demonstrates readily distinguishable peaks of this nature. BP–2MeP is the only one of this series that has a tertiary amide; all the others contain secondary amides. It would appear that the tertiary amide N 1s signal is higher in binding energy than the primary amide, which allows us to distinguish it from the neutral amine N 1s peak. A similar effect is found in the comparison of primary and tertiary alcohol C 1s shifts.[21] The BAC–DMEXA polymer also has two peaks of roughly equal intensity. These are assigned to the (mainly) amide component signal at ~400 eV and the protonated ammonium peak at ~402 eV. Other PAAs, particularly those containing the BAC amide portion demonstrate strong charged ammonium signals. The binding energy positions and component peak areas are listed in Table 6 along with literature values for polyethylenimine (secondary amine), nylon 12 (secondary amide), and poly(vinylbenzene–trimethylammonium chloride) (quaternary ammonium), which are included for comparison.

The level of protonation is worthy of comment since the presence of counterions to the positive nitrogen centers must also be accounted for. We have already noted that the chlorine in these polymers exists as the

Table 6. Binding Energies and Component Peak Areas of the N 1s Region for PAAs

polymer	binding energy (eV)			contribution to N 1s (%)		
	N (amine)	N (amide)	N^+	N (amine)	N (amide)	N^+
BP–2MeP	399.36	400.30		48.2	51.8	
MBA–2MeP	399.73			100		
BAC–2MeP	399.95		402.08	77.9		22.1
MBA–DMEDAsim	399.77		401.81	96.1		3.9
BAC–DMEDAsim	400.01		402.26	65.9		34.1
	399.99		402.26	68.1		31.9
BAC–DMEXA	400.06		402.17	55.9		44.1
	400.08		402.17	53.7		46.3
BAC–DMEDAasim	399.84		402.20	73.7		26.3
	399.85		402.20	72.4		27.6
literature[8]	399.07	399.84	402.14			

anion, and these are almost certainly associated with protonated nitrogen. The presence of zwitterions in polymers with the BAC amide portion may account for some of the cationic nitrogen, and indeed these polymers show a much higher degree of protonation than the three polymers that do not contain BAC. However, it should be noted that these polymers cannot be totally zwitterionic, since that would mean that half of the amines (i.e., 25% of all nitrogen atoms) would be positively charged even discounting the presence of chloride ions. To illustrate this, polymer BAC–2MeP has only 22.1% charged nitrogen atoms. The number of carboxyl anions in the BAC polymers can be estimated by calculating the amount of charged nitrogen countered by chloride ions, the remainder having to be stabilized by the carboxyl groups. Such calculations show that between 60 and 75% of all carboxylic acid groups exist as the anion. Polymer BAC–DMEDAasim demonstrates the highest zwitterionic character, and this may be due to the flexibility of the amine group on the pendant side chain.

All of the O 1s spectra for this series of polymers were similar, with three main features, as demonstrated by the example spectrum in Figure 1e. The main peak appears at 531.61 ± 0.15 eV binding energy for all polymers and demonstrates a shoulder of variable height which has been fitted as a second peak with a binding energy of 532.99 ± 0.20 eV. The main peak contains contributions from the amide group, carboxyl anions, and *O*=COH atoms. These different atoms were not sufficiently separated in binding energy to warrant trying to use individual peaks to represent them. The position and intensity of the second peak varies quite remarkably and is always more intense in the BAC-containing polymers. It may correspond to, or contain contribution from, the O=*C*OH functionality,[8] but this is unlikely to be the whole story since it also appears in the poly(amidoamine)s that do not contain BAC. It is possible that there is also a contribution from retained water, and such an explanation has been used previously to explain a similar feature in the O 1s spectra of poly(*N*-vinylpyrrolidone) and polyacrylamide.[8] The third peak is a low-intensity shakeup satellite, roughly 8 eV higher in binding energy than the main photoelectron signal. Only one peak was used to fit this feature, but there is almost certainly more than one type of shakeup transition possible.

(b) Valence Band Spectra. Valence band spectra for polymers BAC–DMEDAsim, BAC–DMEXA, and BAC–DMEDAasim are shown in Figure 2. It should be noted that BAC–DMEDAsim and BAC–DMEDAasim are isomeric, and their valence band spectra have been overlaid to highlight differences in the spectra. The sharp features that appear at roughly 6 and 17 eV are

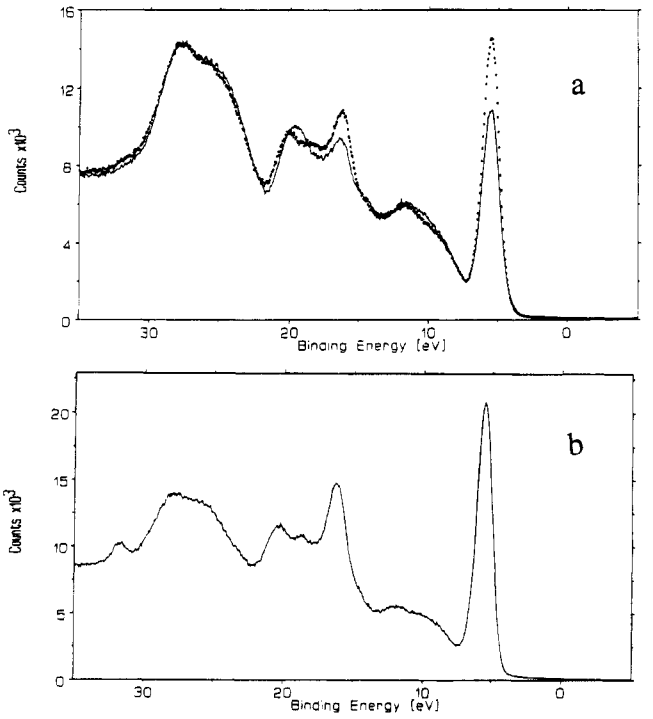

Figure 2. Valence band regions of (dotted line, a) BAC–DMEDAsim, (solid line, a) BAC–DMEDAasim and (b) BAC–DMEXA.

due, respectively, to electrons deriving from the Cl 3p and the Cl 3s orbitals.[8] The intensity of these features is proportional to the concentration of chlorine in the samples, which varies between the polymers in question. The overlapping double peak which appears at 26–28 eV results from both the N 2s and O 2s orbitals.[8] Poly(amidoamine) BAC–DMEXA also demonstrates a small peak at ~32-eV binding energy which is caused by sodium (Na 2p); the wide scan for this polymer did indicate that the polymer contained a small quantity of sodium. The peaks appearing between 17 and 20 eV are the most interesting features of these spectra. This region is dominated by photoelectrons from molecular orbitals containing contributions from mainly C 2s orbitals.[22] The more linear polymers BAC–DMEDAsim and BAC–DMEXA both show a similarity in position and intensity of features, which are two main peaks, one at ~20 eV and a smaller one at ~18 eV. There may be other features in the 17-eV area, but these are obscured by the Cl 3s orbital. By way of contrast, poly(amidoamine) BAC–DMEDAasim has one large peak at ~19-eV binding energy and no other prominent features. The two isomeric polymers in this series can thus be distinguished in the XPS valence band; clearer evidence of their structural differences is seen in the SIMS spectra later in the text. No attempt is made here to explain the differences observed in the valence band spectra of these compounds. This would require calculations which are beyond the scope of this paper.

(c) X-ray Degradation of BAC-Containing Polymers. Three polymers, BAC–DMEDAsim, BAC–DMEXA, and BAC–DMEDAasim were subjected to X-ray irradiation for 10.5 h. During this time three sets of spectra were taken, which comprised (consecutively) a wide scan, narrow scans of all elements, and a valence band spectrum. The first valence band spectra are presented in the preceding section. The valence band spectra took ~2.5 h to collect, and the others took 1 h. The elemental concentrations of the three polymers are plotted against irradiation time in Figure 3. All three polymers exhibit the same trend, dramatic loss of

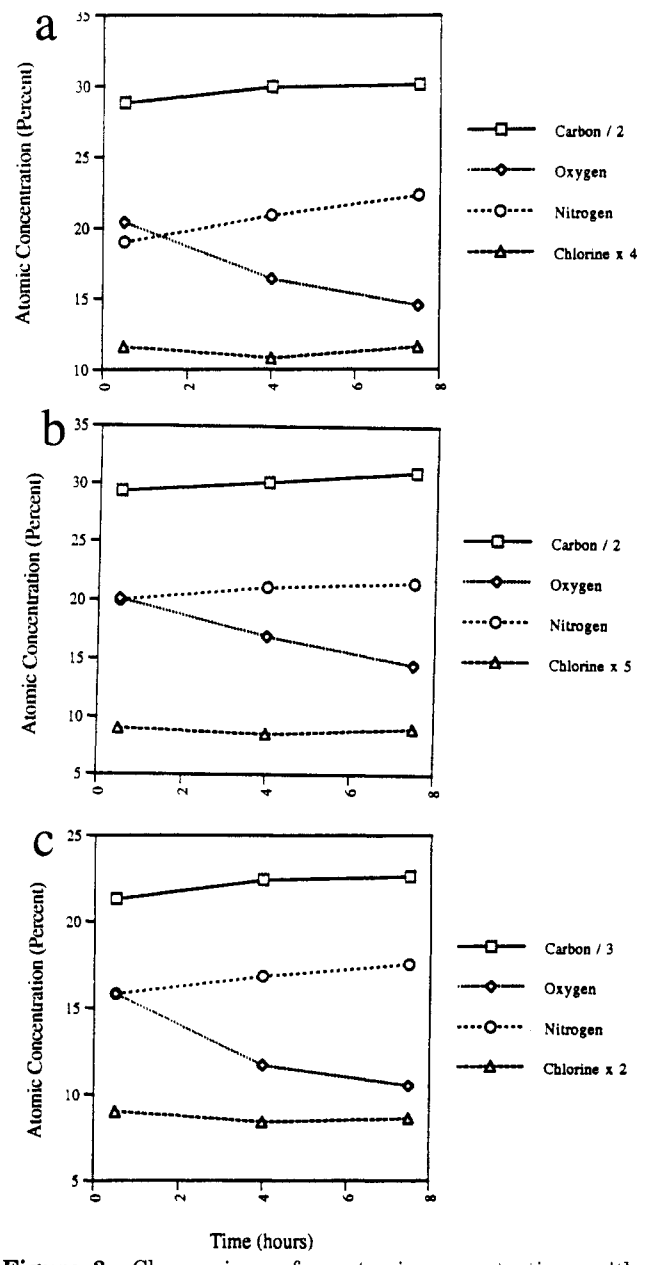

Figure 3. Change in surface atomic concentrations with irradiation time for (a) BAC–DMEDAsim, (b) BAC–DMEDAasim, and (c) BAC–DMEXA.

oxygen while the nitrogen to carbon ratio remains roughly constant; the chlorine content also remains unchanging. The amount of oxygen lost over 7.5-h irradiation is roughly a quarter for the BAC–DMEDA polymers and almost a third for BAC–DMEXA.

Since only oxygen, and not nitrogen, is lost from these polymers, the most obvious degradation route would be the loss of carboxyl groups from the BAC amide portion of the polymers. At the end of 7.5 h half of the carboxyl groups from the BAC–DMEDA polymers and two-thirds of BAC–DMEXA would have to have disappeared. Peak fits of the C 1s envelopes did reveal that all of the components remained in proportion to each other, except for the COO peak, which was reduced by almost half in the case of the BAC–DMEDA polymers and two-thirds in BAC-DMEXA; see Figure 4. A possible mechanism for carboxyl degradation is given below, which involves a simple photoionization followed by loss of carbon dioxide, a process similar to the Kolbe electrolysis.[23]

$$RCOO^- + h\nu \rightarrow RCOO^\bullet + e^- \rightarrow R^\bullet + CO_2$$

The loss of carboxyl groups would be expected to affect

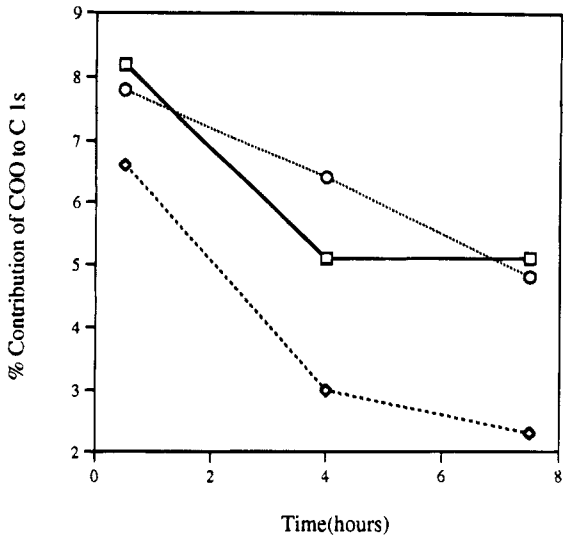

Figure 4. Disappearance of carboxyl groups under X-ray irradiation from BAC–DMEDAsim (squares), BAC–DMEDA-asim (circles), and BAC-DMEXA (diamonds).

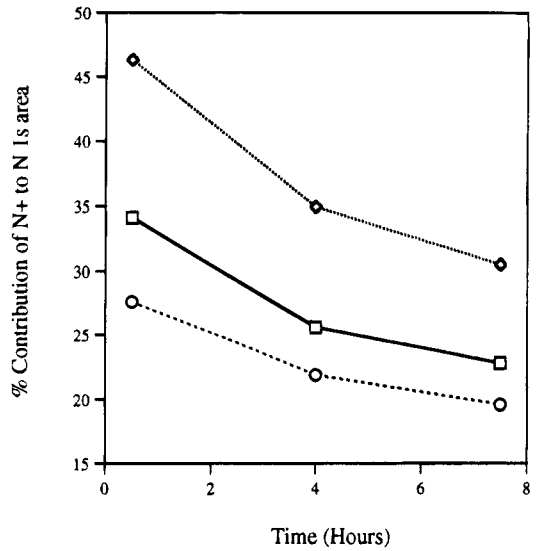

Figure 5. Loss of ammonium groups during irradiation from BAC–DMEDAsim (squares), BAC–DMEDAasim (circles), and BAC–DMEXA (diamonds).

the proportion of nitrogen atoms in a quaternary environment. As Figure 5 shows, this appears to be the case, although such a loss may be due to an isolated photodegradation route affecting only the quaternary ammonium species and not connected to the carboxyl degradation at all. Indeed, the fact that all the polymers demonstrate similar curves and proportions of ammonium loss indicates that the mechanism is probably unrelated to the carboxyl group disappearance.

ToF-SIMS. (a) Positive Ion SIMS Spectra. To aid our understanding of these spectra, we have employed high mass resolution ToF-SIMS on a selected number of poly(amidoamine)s. Typical spectra are presented in Figure 6 along with expanded areas to show multiple peaks appearing at the same nominal mass. Individual peaks arise from differing elemental compositions of fragment ions. Compositions of the fragments can be calculated through a knowledge of isotopic accurate masses and good chemical sense. Representative poly(amidoamine)s chosen were BP–2MeP, MBA–DMEDAsim, BAC–DMEDAsim, BAC–DMEXA, and BAC–DMEDAasim.

(b) C_xN Clusters. We will initially concentrate on fragment ions containing one nitrogen atom with carbon and hydrogen. The maximum number of carbon atoms attached to one nitrogen atom can be readily determined from the structures of the individual poly(amidoamine)s. For convenience we are ignoring the possibility of elimination or rearrangement reactions which may increase the number of carbon atoms attached to one nitrogen. The values in Table 7 are normalized intensity (to 100%) over the C_xN group, so that comparison can easily be made between different polymers. The number in parentheses next to these values is the absolute peak intensity expressed as a percentage of the most intense peak in the spectrum. It should be noted that some of these peaks are not the most intense that appear at their nominal mass values, but the high-resolution spectra allow them to be separated from the more intense ions.

All polymers showed fragments containing one nitrogen atom with all possible numbers of carbon atoms up to the maximum predicted. All polymers also demonstrated an ammonium ion in weak intensity at *m/z* 18. The polymers MBA–DMEDAsim and BAC–DMEDA-asim also exhibited weak ions in the C_6N cluster which are difficult to explain from a straightforward fragmentation process. These are labeled with question marks in the table. It is possible that some rearrangement occurred which lead to their formation. The proposed structures of the highest mass observed single nitrogen species are given below (except for MBA–DMEDAsim). Other fragments can be assigned to similar species. The number of possible structures (i.e., length of carbon chains, location of double bonds) for some ions is quite large and we think that almost all make some contribution to the observed peak.

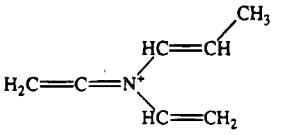

m/z 108 BP-2MeP

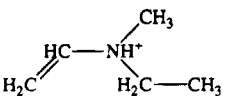

m/z 86 BAC-DMEDAsim

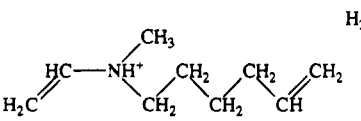

m/z 140 BAC-DMEXA

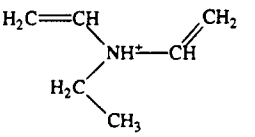

m/z 98 BAC-DMEDAasim

A comparison of ion intensities within each individual cluster leads to some interesting observations. It can be seen that within the C_3N, C_4N, and C_5N clusters both polymers containing the DMEDAsim diamine unit exhibit closely similar distributions of ions. This is to be expected since the ions are being produced from the same structural unit. There is, however, a tendency, especially in the C_2N cluster (and marked in the C_3N cluster), for the BAC-containing polymer to produce more intense peaks with a higher hydrogen content. This is probably related to the degree of quaternization (see XPS results). MBA–DMEDAsim has one of the lowest quaternary ammonium contents of all the polymers. The BAC polymers have higher amounts of protonated nitrogen, and this increases the number of routes to ion formation as, for example, shown below. As this reaction scheme demonstrates, a higher degree of protonation leads to a higher production of the *m/z* 44 ion through the concerted route shown at the bottom. Neutral amines would tend to produce uncharged fragments through this reaction. Increasing the amount of

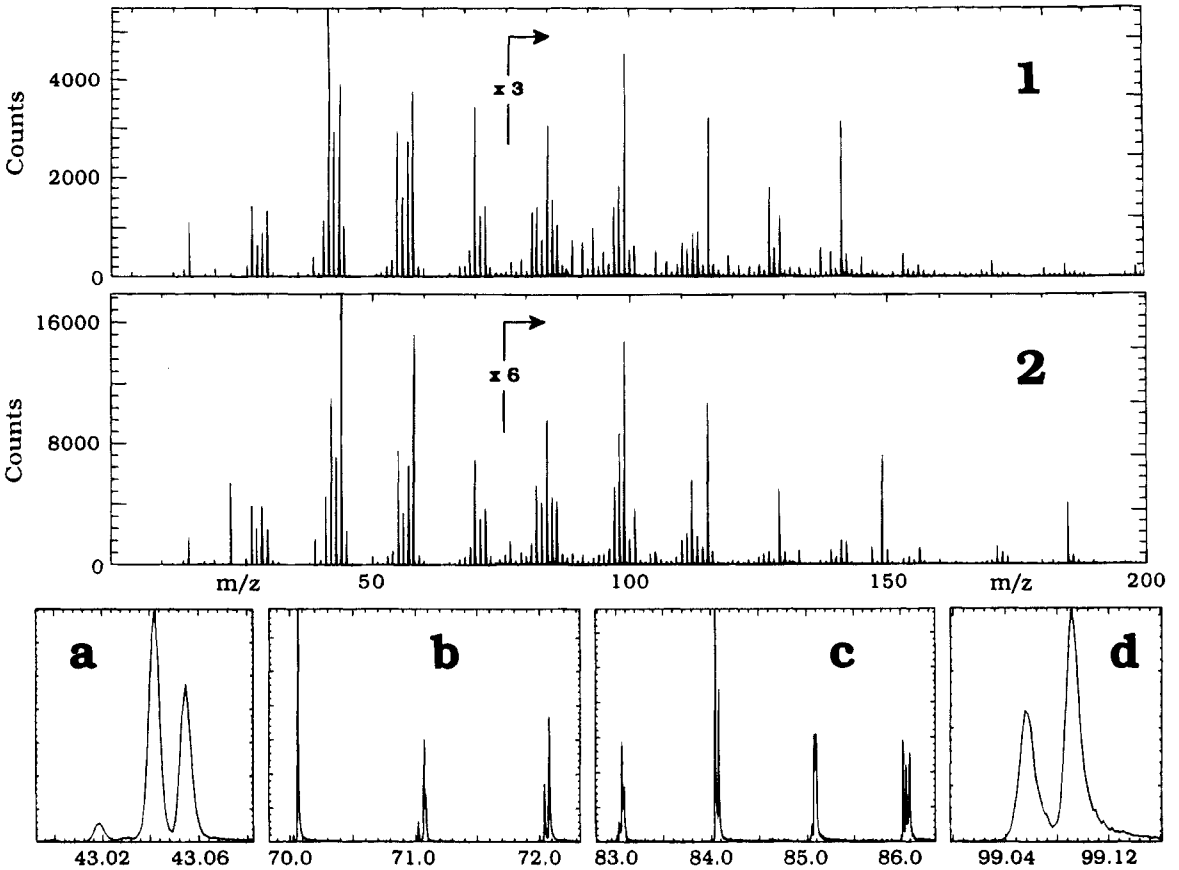

Figure 6. High mass resolution positive ion ToF-SIMS spectra (*m/z* 0–200) recorded for MBA–DMEDAsim (1) and BAC–DMEDAsim (2) with expansions for BAC–DMEDAsim at (a) *m/z* 43, (b) 70–72, (c) 83–86, and (d) 99.

quaternary ammonium causes a rise in intensity of the *m/z* 44 ion; BAC–DMEXA, which had the highest quaternary ammonium signal in the XPS data, has over 60% of the C_2N cluster intensity within the *m/z* 44 ion.

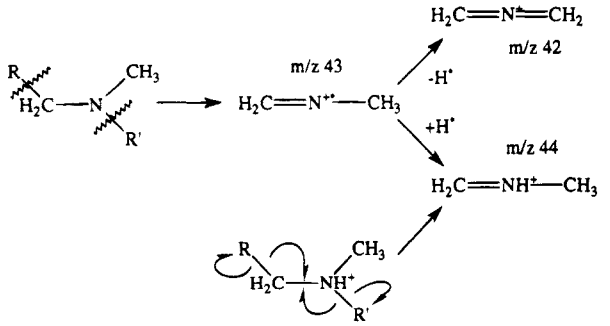

Within the CN cluster, the MBA–DMEDAsim polymer demonstrates a trend the reverse of that of the C_2N cluster and has a more intense higher mass ion at *m/z* 30. All of the BAC-containing polymers have roughly equivalent *m/z* 28 and 30 intensities, which are thought to derive from the $RN(CH_3)R'$ unit. The explanation in this case must be due to the MBA amide section $RCONH–CH_2–NH–OCR$ fragmenting preferentially to give $H_2C{=}NH_2^+$, in the same way, perhaps, as nylons, which are aliphatic polyamides, where the SIMS spectra also demonstrate a higher *m/z* 30 compared to *m/z* 28 intensity.[24]

Routes to C_xN ion production in the BAC–DMEXA poly(amidoamine) appear to be somewhat similar (at least up until C_5N) to BAC–DMEDAsim since the cluster intensities follow the same trends. The spectrum of the isomeric polymer BAC–DMEDAasim is vastly different from any of the other polymers. At least three features stand it out from the other polymers: the intense radical cation $C_2H_7N^{\bullet+}$ and the two intense peaks $C_3H_8N^+$ and $C_4H_{10}N^+$, which both make up over 80% of the intensity of their respective clusters and are the two most intense peaks in the spectrum. All of these ions derive from the polymer side chain, as shown below. Their high intensities are due to an easier formation of ions resulting from single-bond cleavages compared to at least two for similar ions from other polymers. In fact the rest of the spectrum was so weak (compared to other polymers in this series) that it seems that loss of these pendant groups accounts for a large proportion of the energy dissipation following ion bombardment in this polymer.

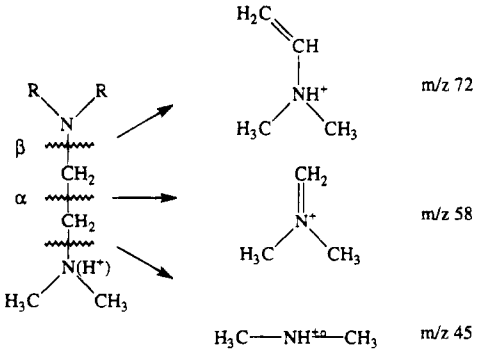

The distribution of C_xN peaks in the BP–2MeP poly(amidoamine) SIMS spectrum (low-resolution spectrum shown in Figures 7a and 8a) bears little resemblance to any of the other polymers. This is to be expected since it is structurally very different. The amine portion is cyclic and it also contains a cyclic amide that may contribute fragment ions up to the C_4N cluster. In general, there is a tendency for the peak distribution of each cluster to be concentrated at a lower mass than

Table 7. Ions Containing One Nitrogen Atom from High Mass Resolution ToF-SIMS

Fragment	BP–2MeP	MBA–DMEDAsim	BAC–DMEDAsim	BAC–DMEXA	BAC–DMEDAasim
CN cluster					
28 CH_2N^+	56 (25.2)	28 (9.9)	45 (13.2)	44 (9.6)	47 (3.6)
29 $CH_3N^{\bullet+}$	8 (3.8)	4 (1.5)	7 (2.1)	7 (1.6)	7 (0.5)
30 CH_4N^+	36 (16.0)	67 (23.7)	44 (12.9)	42 (9.2)	43 (3.3)
31 $CH_5N^{\bullet+}$	(0.2)[a]	1 (0.5)[a]	4 (1.4)	7 (1.6)	3 (0.2)
C_2N cluster					
41 $C_2H_3N^{\bullet+}$	8 (11.3)	2 (4.2)	2 (3.4)	2 (3.0)	2 (0.9)
42 $C_2H_4N^+$	70 (100.0)	43 (100.0)	30 (61.3)	25 (42.4)	34 (13.0)
43 $C_2H_5N^{\bullet+}$	10 (14.3)	23 (52.6)	19 (38.8)	12 (19.4)	9 (3.3)
44 $C_2H_6N^+$	12 (17.2)	31 (71.2)	48 (100.0)	60 (100.0)	41 (16.0)
45 $C_2H_7N^{\bullet+}$	(0.3)[a]	1 (2.5)[a]	1 (3.1)[a]	2 (3.1)[a]	14 (5.4)
C_3N cluster					
54 $C_3H_4N^+$	13 (23.5)	4 (6.1)	3 (5.1)	5 (2.8)	1 (1.5)
55 $C_3H_5N^{\bullet+}$	16 (27.6)	3 (4.4)	2 (3.7)	3 (1.9)	1 (1.5)
56 $C_3H_6N^+$	54 (93.9)	14 (22.1)	13 (19.1)	12 (7.5)	7 (8.6)
57 $C_3H_7N^{\bullet+}$	10 (17.6)	31 (48.2)	24 (35.8)	32 (19.5)	3 (3.6)
58 $C_3H_8N^+$	7 (12.6)	46 (70.6)	56 (86.3)	46 (28.0)	84 (100.0)
59 $C_3H_9N^{\bullet+}$	(0.5)[a]	2 (2.7)[a]	2 (3.2)[a]	2 (1.2)[a]	4 (4.4)[a]
C_4N cluster					
66 $C_4H_4N^+$	1 (1.2)	– (0.4)	1 (0.5)	2 (0.5)	
67 $C_4H_5N^{\bullet+}$	1 (1.5)	1 (0.8)	1 (0.5)	2 (0.5)	
68 $C_4H_6N^+$	17 (17.8)	3 (3.7)	3 (2.8)	8 (2.7)	1 (0.8)
69 $C_4H_7N^{\bullet+}$	27 (29.4)	1 (0.8)	– (0.3)	1 (0.3)	1 (0.4)
70 $C_4H_8N^+$	40 (44.2)	53 (62.8)	48 (40.3)	51 (16.9)	5 (3.5)
71 $C_4H_9N^{\bullet+}$	9 (9.2)	19 (23.0)	21 (17.4)	19 (6.5)	6 (4.1)
72 $C_4H_{10}N^+$	5 (5.9)	22 (25.7)	25 (20.7)	16 (5.2)	82 (52.2)
73 $C_4H_{11}N^{\bullet+}$	(0.5)	1 (1.4)[a]	1 (1.1)[a]	1 (0.3)[a]	5 (3.0)[a]
C_5N cluster					
80 $C_5H_6N^+$	11 (4.3)	2 (0.6)	3 (0.4)	3 (0.6)	11 (0.3)
82 $C_5H_8N^+$	36 (13.6)	37 (8.6)	30 (3.8)	16 (2.8)	32 (0.9)
83 $C_5H_9N^{\bullet+}$	3 (1.1)	4 (0.9)	2 (0.3)	7 (1.3)	
84 $C_5H_{10}N^+$	47 (17.5)	40 (9.4)	38 (4.9)	58 (10.5)	43 (1.2)
85 $C_5H_{11}N^{\bullet+}$			5 (0.7)	5 (0.9)	
86 $C_5H_{12}N^+$	3 (1.1)	17 (3.9)	22 (2.8)	11 (2.0)	14 (0.4)
C_6N cluster					
92 $C_6H_6N^+$	8 (1.8)				
94 $C_6H_8N^+$	18 (3.9)	28 (1.1)?	22 (0.4)?	7 (0.8)	29 (0.2)
96 $C_6H_{10}N^+$	31 (7.0)	39 (1.5)?	45 (0.8)?	17 (1.9)	42 (0.3)
98 $C_6H_{12}N^+$	43 (9.6)	33 (1.3)?	33 (0.6)?	62 (7.2)	29 (0.2)
100 $C_6H_{14}N^+$				14 (1.7)	
C_7N cluster					
108 $C_7H_{10}N^+$	100 (1.9)			6 (0.4)	
110 $C_7H_{12}N^+$				19 (1.2)	
112 $C_7H_{14}N^+$				53 (3.4)	
114 $C_7H_{16}N^+$				22 (1.4)	
C_8N cluster					
124 $C_8H_{14}N^+$				28 (1.3)	
126 $C_8H_{16}N^+$				61 (2.8)	
128 $C_8H_{18}N^+$				11 (0.5)	
C_9N cluster					
140 $C_9H_{18}N^+$				100 (0.3)	

[a] Contains a significant contribution from ions with one less hydrogen atom and a ^{13}C carbon atom.

all of the other polymers. This cannot be ascribed solely to a low degree of quaternization, since MBA–DMEDAsim possesses a similar degree of protonation. More probably, greater unsaturation in the fragments is caused by more bonds (i.e., three compared to, in general, two) having to be broken to produce a C_xN ion from BP–2MeP.

(c) C_xN_2 Clusters. All of the polymers except for Bp–2MeP demonstrated a $CH_5N_2^+$ *m/z* 45 ion, which is formed from a fragmentation of the amide section of the polymer. The equivalent ions from the BP–2MeP amide appear mainly at *m/z* 83 and 85 due, respectively, to the $C_4H_7N_2^+$ and $C_4H_9N_2^+$ ions. Polymer BAC–DMEXA demonstrated only the *m/z* 45 ion and three ions in weak intensity at *m/z* 138, 139, and 155, respectively, due to $C_8H_{14}N_2^{\bullet+}$, $C_8H_{15}N_2^+$, and $C_9H_{19}N_2^+$. Ions from this PAA containing just hydrogen, oxygen, and two nitrogen atoms at lower mass than this are not observed, which, considering the polymeric structure, is suggestive that simple fragmentation processes can explain the appearance of these ions.

The DMEDA-containing polymers give quite similar distributions of ion intensities throughout the clusters where they are present (C_2N_2 to C_7N_2). From the structures of the polymers it is possible only to envisage a maximum of eight carbon atoms being attached to two nitrogen atoms from these polymers. However, only BAC–DMEDAsim produced an ion of sufficient intensity to be positively identified at *m/z* 139. Some slight differences in relative ion intensities in each cluster may be noted, especially between the symmetric and nonsymmetric BAC–DMEDA polymers at lower mass. In general, the BAC–DMEDAasim polymer produces more intense ions in each cluster at higher mass; for instance, in the C_5N_2 cluster the *m/z* 101 signal due to $C_5H_{13}N_2^+$ accounts for nearly a third of the cluster intensity with the $C_5H_{11}N_2^+$ ion in roughly equal intensity. In the spectra of polymers MBA–DMEDAsim and BAC–DMEDAsim, over half of the cluster intensity is due to the latter ion, with the *m/z* 97 $C_5H_9N_2^+$ ion being more intense than the *m/z* 101 ion. These variations can be ascribed to the differing structure of DMEDA symmetric and assymmetric PAAs.

The clusters of C_5N_2 and above in the polymer BP–2MeP are produced from the diamine ring. It is possible to envisage fragment clusters up to C_9N_2 from the polymeric structure. We do indeed observe peaks at *m/z* 151 and 153 that belong to this cluster and no others

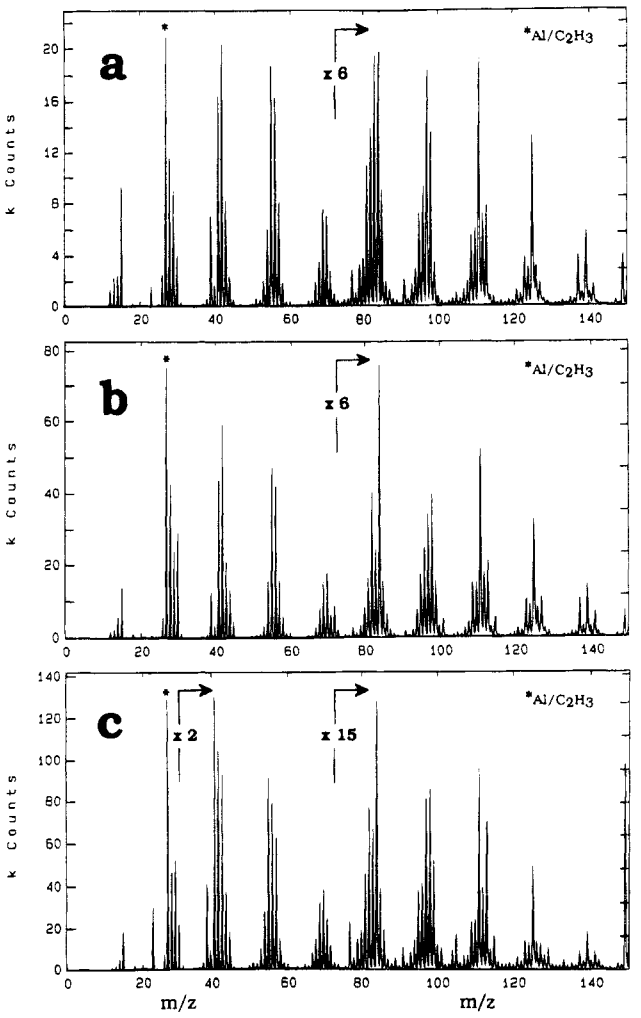

Figure 7. Positive ion ToF-SIMS spectra (m/z 0–150) recorded for (a) BP–2MeP, (b) MBA–2MeP, and (c) BAC–2MeP.

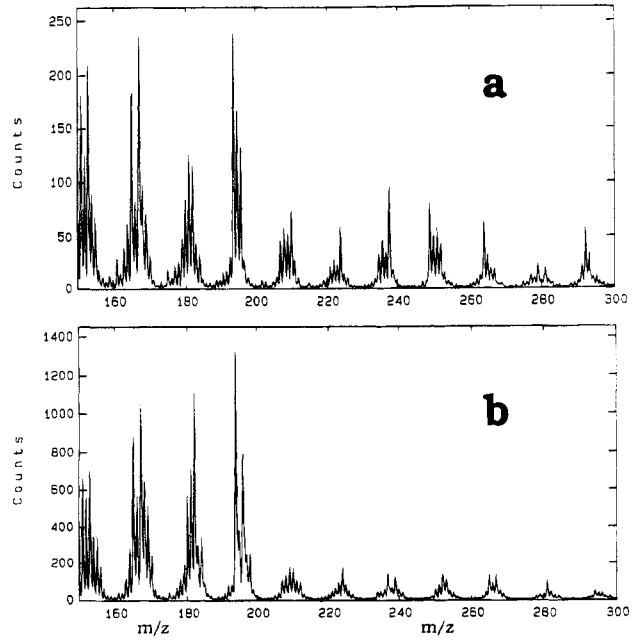

Figure 8. Positive ion ToF-SIMS spectra (150–300) recorded for (a) BP–2MeP and (b) MBA–2MeP.

beyond that. The proposed structures for some of the high-mass and other intense ions are

(d) Oxygen-Containing Ions. Many peaks were also observed which contained at least one oxygen atom. Intense peaks were seen in most polymers at low mass which were due to species such as $C_2H_3O^+$, $C_2H_5O^+$,

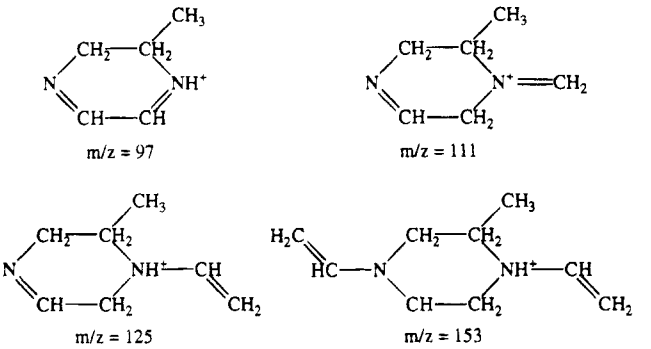

$C_3H_3O^+$, and $C_3H_5O^+$. Such ions can be formed from the $R_2N-C(O)-CH_2-CH_2-NR_2$ section, which is common to all of the polymers. Cleavage of the amide C–N bond to produce an ion containing both the amide oxygen and at least one amine nitrogen should give easily identifiable ions. Caution must be used, however, since fragments that contain the complete amide may exist.

The most useful comparison to be made is between polymers MBA–DMEDAsim and BAC–DMEDAsim. Both of these polymers show a good number of common ions. The only structural difference between the two is a carboxylic acid group in the amide section of the BAC polymer. Large differences in ion intensity can thus be ascribed to the influence of the carboxylic acid group. MBA–DMEDAsim has four very intense ions at m/z 115, 127, 129, and 141 which correspond to ions $C_5H_{11}N_2O^+$, $C_6H_{11}N_2O^+$, $C_6H_{13}N_2O^+$, and $C_7H_{13}N_2O^+$ (respective relative intensities 20.2, 10.6, 7.2, and 19.8). BAC–DMEDAsim only has strong signals at m/z 115 and 129 (relative ion intensities—as before—8.7, 0.7, 4.0, and 1.3). The simplest explanation for this observation is in the following series of assignments, all of which contain an intact amide bond. It is difficult to envisage a sensible assignment for the m/z 115 ion, which derives from a broken C–N amide link, and since this ion is so intense in both polymers, it is assumed that the slightly weaker m/z 129 ion has a similar structure. BAC–DMEXA and BAC–DMEDAasim produced much weaker ions in this series.

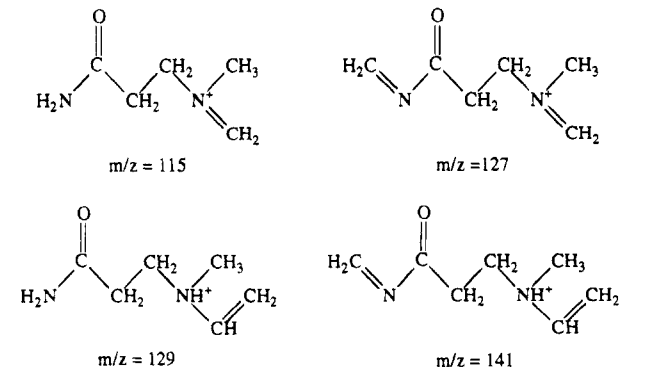

Intense ions appear in both polymers that can be formed from an amide bond cleavage. The series of ions at m/z 72, 84, 98, and 112 belong to a series of $C_xH_yNO^+$ ions which, at least beyond $C_4H_6NO^+$, must come from an amide bond cleavage. The relative intensities for BAC–DMEDAsim are, respectively, 9.7, 7.9, 7.2, and 4.5, whereas for MBA–DMEDAsim they are 20.9, 18.9, 11.5, and 5.5. An example structure for m/z 112 is given below along with the largest feasible ion containing an intact amide bond (m/z 84). The polymers BAC–DMEXA and BAC–DMEDAasim also produced ions in this series with relative intensities for the former of 2.6,

4.0, 1.7, and 0.1, respectively, and for the latter, 1.7, 2.4, 1.3, and 0.5.

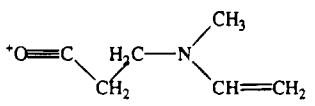

m/z = 112

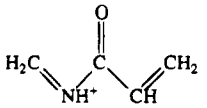

m/z = 84

Poly(amidoamine) BP–2MeP gave few intense ions which contained a single oxygen atom. Ions at *m/z* 70, 84, and 98 due to $C_xH_{2x-2}NO^+$ species appeared in roughly equal intensities (6.0, 6.4, and 5.4 relative to the main peak, respectively). An isolated ion at *m/z* 113, which has the composition $C_5H_9N_2O^+$, may be explained by an ion containing the complete amide ring; see below. Ions also appear at *m/z* 139/141, 151/153, and 165/167. The first pair of ions probably results from the amide portion of the polymer, a proposed structure is shown below. The second two ion pairs almost certainly derive from fragments containing a complete amine ring; the structure of the *m/z* 153 ion is shown below also.

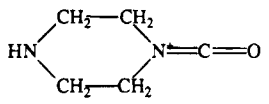

m/z = 113

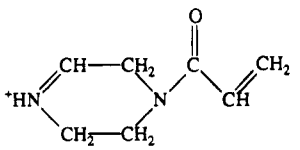

m/z = 139

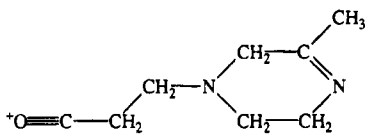

m/z = 153

At higher mass number, polymer BP–2MeP also gives a series of prominent peaks which are identified as the $C_xH_yN_3O$ series at *m/z* 181, 182, 194, and 196. Also peaks at *m/z* 195 and 238 identified as the $C_{10}H_{15}N_2O_2^+$ and $C_{12}H_{20}N_3O_2^+$ ions are evident.

A number of relatively weak ions at low mass (below *m/z* 150) and slightly stronger ions at higher mass in the BAC-containing polymers appear to contain complete or partial carboxylic acid groups. These are ions that comprise, in general, at least two oxygen atoms. The spectrum that demonstrates these most strongly is the BAC–DMEDAsim, and the following discussion will be based around ions appearing in that spectrum. An ion with reasonable intensity (3.4% of the base peak) appears at *m/z* 86; this has the formula $C_3H_4NO_2^+$ and must derive from the diamide link. Similarly, the series of ions at *m/z* 125, 127, and 129 (intensities 0.1, 0.1, and 0.7, respectively) due to the $C_5H_xN_2O_2^+$ ions also come from this linking unit. An ion at *m/z* 128 has an atomic composition of $C_5H_6NO_3^+$ and contains the complete carboxylic acid group. Finally, some relatively intense ions (given their high mass) appear at *m/z* 171, 173, and 185 (intensities 0.9, 0.4, and 3.3) and at *m/z* 214, 228, and 242 (intensities 0.4, 0.2, and 0.8) which are due to, first, the $C_xH_yN_2O_3^+$ series and the $C_xH_{2x-4}N_3O_4^+$ series. Example structures are

Poly(amidoamine) MBA–DMEDAsim gave strong high-mass peaks at *m/z* 170, 184, 198, and 212 (intensities, respectively, 2.0, 1.6, 1.3, and 0.9). These ions had the general formula $C_xH_{2x-2}N_3O_2^+$, and the first three are exactly analogous to the *m/z* 214–242 species seen in BAC–DMEDAsim, without the carboxyl group (i.e., 44 amu less).

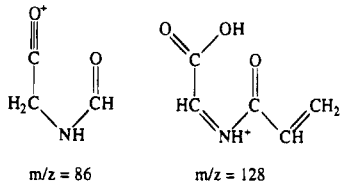

m/z = 86

m/z = 128

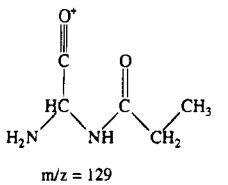

m/z = 129

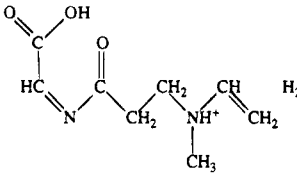

m/z = 185

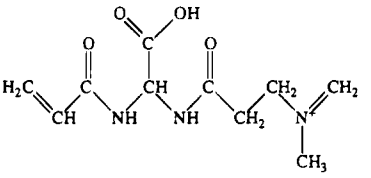

m/z = 242

While signals characteristic of common contaminants such as phthalate and poly(dimethylsiloxane) were discernable in most of the high mass resolution spectra, overall the ToF-SIMS data are consistent with very clean polymer surfaces, in agreement with the XPS results. It must be noted that ToF-SIMS is a very sensitive analytical technique for many organic and inorganic species, including phthalate and silicone. Furthermore, it should be emphasized that the general analytical sensitivity of ToF-SIMS is greatly enhanced with high mass resolution in view of the fact that detection limits are often restricted by mass overlap.

(e) 2-Methylpiperazine PAAs. The results we have acquired thus far can be used to interpret the ToF-SIMS spectra of poly(amidoamine)s MBA–2MeP and BAC–2MeP. The spectra for these are shown in Figures 7 and 8 along with that of the BP–2MeP polymer for comparison. It should be noted that all polymers display a peak at *m/z* 149 which is assigned to a phthalate contaminant.[25]

The size and distribution of peaks below *m/z* 60, especially for the BP- and MBA-containing polymers, are very similar, the first real difference occurring in the cluster of ions at *m/z* ~70. It can be seen that the BP polymer has prominent *m/z* 69 and 70 peaks. The former is due to a roughly equal combination of the $C_5H_9^+$ and $C_4H_7N^{\bullet+}$ ions, whereas the latter is almost solely the result of the $C_4H_8N^+$ ion. This is found to be the case also for the BAC polymer, but the MBA-containing poly(amidoamine) has quite a strong *m/z* 72 ion, which can be ascribed to the $C_3H_6NO^+$ species also seen in MBA–DMEDAsim. The next cluster at *m/z* ~82 carries prominent odd mass signals in the case of the BP polymer. Signals at *m/z* 83 and 85 had large contributions from the $C_4H_7N_2^+$ and $C_4H_9N_2^+$ which were thought to derive from the BP amide group. These two peaks are much smaller by comparison with the *m/z* 82 and 84 peaks in the MBA- and BAC-containing polymers which implies that the origin of these two ions was correctly identified. Within the cluster appearing around *m/z* 98 it can be seen that the BP polymer has *m/z* 97 due to the diamine $C_5H_9N_2^+$ as the most intense peak. Although both of the other 2MeP poly(amidoamine)s display this peak, the *m/z* 98 peak appears to be stronger. The increase in this intensity may be due to the $C_5H_8NO^+$ and/or the $C_6H_{12}N^+$ ions. Why these should be more intense in the MBA and BAC polymers is unknown.

Between *m/z* 100 and 150 there are great similarities again between the three polymers. The prominent ions at and around *m/z* 111, 125, and 139 have been discussed previously. Both polymers MBA–2MeP and BAC–2MeP display moderate ion intensities at *m/z* 115. These features do not appear in the BP-PAA, but the

m/z 115 does in MBA–DMEDAsim where it was due to $C_5H_{11}N_2O^+$. Also appearing in that series were ions at *m/z* 127, 129, and 141. Slightly enhanced intensities at *m/z* 127 and 141 can be seen in the MBA and BAC polymers compared to BP–2MeP, but *m/z* 129 is only slightly enhanced in the case of BAC–2MeP. All of these changes are rather subtle, and it is obvious that these ions are not of major importance to the spectra of the 2MeP compounds; they require the scission of three bonds to form which perhaps accounts for their low intensity.

Above *m/z* 150, the BAC spectrum becomes very weak and is not worth discussing in detail. However, this is where the differences between the BP–2MeP and MBA–2MeP polymers start to become apparent, as shown in Figure 8. Both spectra show the *m/z* 151/153 and 165/167 ions previously discussed and also a similar cluster around *m/z* 181. The *m/z* 182 ion is very intense here for the MBA–2MeP polymer; its mass indicates an odd number of nitrogen atoms. By virtue of the fact that there are also prominent species at *m/z* 194, 196, and 208 (the *m/z* 208 is not so clear) and analogy to the recently discussed DMEDAsim series at *m/z* 115, 127, 129, and 141, these ions have been assigned to the example structures given below. The BP polymer also shows these ions, along with an enhanced *m/z* 195 ion which is assigned to the amide ring as shown below.

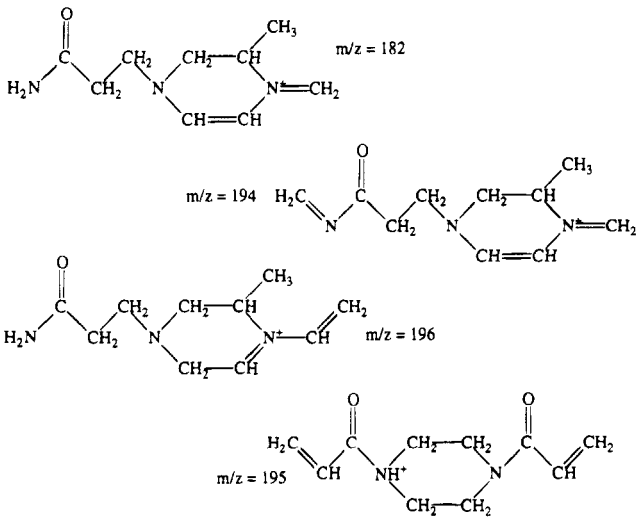

Above *m/z* 200, the two polymers BP–2MeP and MBA–2MeP demonstrate some substantial differences in ion intensities. Both polymers show a strong ion corresponding to the $[M - 2H]^{\bullet+}$ radical cation at *m/z* 252 for the MBA polymer and *m/z* 292 for the BP polymer. There are numerous assignments that can be made for these species, and it is unclear which are the more likely. By analogy to the high-mass ions found in MBA–DMEDAsim, a number of assignments of prominent ions may be made to account for many of the features observed in these spectra. It should be noted that both of the polymers demonstrate peaks at *m/z* 224 and 210 in quite large intensity, which may be explained by ions containing the complete 2MeP ring with parts of both amide groups attached to it on either side (e.g., *m/z* 196 shown above plus CO = *m/z* 224).

(f) Negative Ion SIMS Spectra. The negative ion spectra of these polymers were less informative than the positive ion spectra. Almost all the intensity was concentrated at low mass; see examples in Figure 9. The polymers demonstrated strong ions corresponding to C_n^- and C_nH^- at *m/z* 12, 13, 24, and 25, also O^- and OH^-

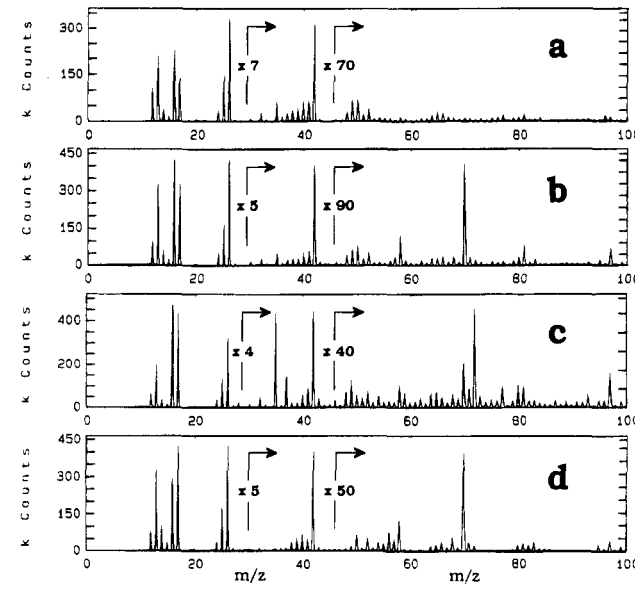

Figure 9. Negative ion ToF-SIMS spectra (*m/z* 0–100) recorded for (a) BP–2MeP, (b) MBA–2MeP, (c) BAC–2MeP, and (d) MBA–DMEDAsim.

at *m/z* 16 and 17 and an intense peak at *m/z* 26 from the CN^- ion. Those poly(amidoamine)s which contained chloride ions produced signals at *m/z* 35 and 37 from the isotopic ions of Cl^-. A further ion at *m/z* 42 is ascribed to the isocyanate ion OCN^- from the amide group. All of the polymers apart from BP–2MeP produced a relatively strong ion signal at *m/z* 70 due to the $CH_2{=}CHCONH^-$ ion. This ion is only formed in large intensity in these polymers from a secondary amide; the tertiary amide in BP-2MeP does not exhibit it. All polymers containing the BAC unit, with a carboxylic acid group, also exhibited a relatively intense signal at *m/z* 72 corresponding to the $NH{=}CHCOO^-$ ion. At higher mass, not shown, there were notable peaks at *m/z* 170 for MBA–2MeP and *m/z* 158 for MBA–DMEDAsim. These are assigned to the structures below. Both of these polymers, as demonstrated by XPS, contain very few protonated amine groups and this may explain why similar ions are not observed in the BAC–2MeP and BAC–DMEDAsim PAAs. If the amine groups were protonated in the fragment, this would result in an overall neutral or singly positive charge on these species, making them undetectable in the negative ToF-SIMS mode.

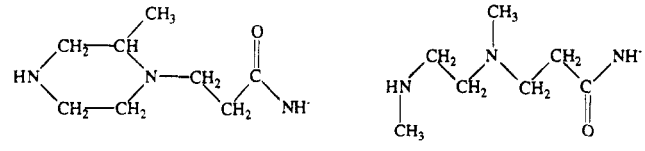

Conclusions

We have described the analysis of poly(amidoamine)s by XPS in detail and found the surface of these polymers within the XPS sampling depth to be almost identical to the bulk stoichiometry. We have noted that the levels of quaternary amine in some of these polymers is much higher than can be accounted for from the amount of chlorine present and have demonstrated that it is likely that zwitterionic moieties exist in such poly(amidoamine)s. Additionally, we have indicated the likelihood of strongly bound water in these polymers.

Valence band spectra were collected from three of the poly(amidoamine)s, and significant differences were found to occur in these between the two isomeric polymers BAC–DMEDAsim and BAC–DMEDAasim. Furthermore, these polymers were subjected to long-term X-ray exposure and found to degrade quite rapidly, losing the carboxylic acid group from the amide portion of the polymer.

High mass resolution ToF-SIMS analyses of these compounds permitted the unambiguous assignment of many of the spectral peaks. In addition, the distinction of each component peak that contributes to individual *m/z* values enables a detailed interpretation of the relationship between polymeric structure and SIMS spectra. We have shown how the intensity of nitrogen-containing fragment clusters may be used to indicate not only the structure of the polymer but also the degree of quaternization. In general, it is found that in these polymers it is unnecessary to invoke complex reaction pathways to explain the appearance of almost all the observed ions; simple fragmentations involving one to three cleaved bonds may be employed.

The work presented here will be invaluable to future studies of systems which contain PAAs, in particular those devices intended for biomedical application in which the presence of these polymers at the material surface is necessary. In addition, we feel that the ToF-SIMS data and detailed interpretation will be of benefit to workers who are using similar techniques to study organic materials containing amine or amide functionalities. We have demonstrated that complex SIMS spectra from polymers like PAAs can be rationalized through the use of high resolution ToF-SIMS.

Acknowledgment. This work was funded by BRITE-Euram program 5706 and the EPSRC.

References and Notes

(1) Ferruti, P.; Marchisio, M. A.; Barbucci, R. *Polymer* **1985**, *26*, 1336, and references therein.
(2) Marchisio, M. A.; Longo, T.; Ferruti, P. *Experientia* **1973**, *29*, 93.
(3) Marchisio, M. A.; Ferruti, P.; Bertoli, S.; Barbiano di Belgiojoso, G.; Samour, C. M.; Wolter, K. D. *Experientia* **1973**, *29*, 39.
(4) Barbucci, R.; Benvenuti, M.; Dal Maso, G.; Ferruti, P.; Nocentini, M.; Russo, R.; Tempesti, F.; Duncan, R.; Bridges, J. F.; McCormick, L. A. In *Polymers in Medicine III*; Migliaresi, C., Nicolais, G. P., Giusti, P., Chiellini, F., Eds.; Elsevier: Amsterdam, 1988.
(5) Ferruti, P.; Ranucci, E.; Sartore, L.; Marchisio, M. A.; Veronese, F. M. In *Macromolecules 1992*; Kahovec, J., Ed.; VSP Intern. Science Publishers: Zeist, The Netherlands, 1993; p 251.
(6) Ranucci, E.; Spagnoli, G.; Ferruti, P.; Sgouras, D.; Duncan, R. *J. Biomater. Sci., Polym. Ed.* **1991**, *2*, 303.
(7) Davies, M. C.; Short, R. D.; Khan, M. A.; Watts, J. F.; Brown, A.; Eccles, A. J.; Humphrey, P.; Vickerman, J. C.; Vert, M. *Surf. Interface Anal.* **1989**, *14*, 115.
(8) Beamson, G.; Briggs, D. *High Resolution XPS of Organic Polymers. The Scienta ESCA300 Database*; Wiley: Chichester, U.K.,
(9) de Matteis, C. I.; Davies, M. C.; Leadley, S.; Jackson, D. E.; Beamson, G.; Briggs, D.; Heller, J.; Franson, N. M. *J. Electron Spectrosc. Relat. Phenom.* **1993**, *63*, 221.
(10) Davies, M. C.; Khan, M. A.; Domb, A.; Langer, R.; Watts, J. F.; Paul, A. J. *J. Appl. Polym. Sci.* **1991**, *42*, 1597.
(11) Bignotti, F.; Sozzani, P.; Ranucci, E.; Ferruti, P. *Macromolecules* **1994**, *27*, 7171–7178.
(12) Beamson, G.; Briggs, D.; Davies, S. F.; Fletcher, I. W.; Clark, D. T.; Howard, J.; Gelius, U.; Wannberg, B.; Baltzer, P. *Surf. Interface Anal.* **1990**, *15*, 541.
(13) Gelius, U.; Wannberg, B.; Baltzer, P.; Fellner-Feldegg, H.; Carlsson, G.; Johansson, C.-G.; Larsson, J.; Münger, P.; Vegerfors, G. *J. Electron. Spectrosc. Relat. Phenom.* **1990**, *52*, 747.
(14) Eccles, A. J.; Vickerman, J. C. *J. Vac. Sci. Technol.* **1989**, *A7*, 234.
(15) Briggs, D.; Hearn, M. J. *Vac.* **1986**, *36*, 1005.
(16) Reichmaier, S.; Hammond, J.; Hearn, M. J.; Briggs, D. *Surf. Interface Anal.* **1994**, *21*, 739.
(17) Briggs, D.; Seah, M. P. *Practical Surface Analysis*, Vol. 1. *Auger and X-ray Photoelectron Spectroscopy*, 2nd ed.; Wiley: Chichester, U.K., 1990.
(18) Jahn, P. W.; Petrat, F. M.; Wolany, D.; Deimel, M.; Gantenfort, T.; Schmerling, C.; Wensing, H.; Wiedmann, L.; Benninghoven, A. *J. Vac. Sci. Technol.* **1994**, *A12*, 671.
(19) Chehimi, M. M.; Watts, J. F.; Eldred, W. K.; Fraoua, K.; Simon, M. J. *Mater. Chem.* **1994**, *4*, 305.
(20) Roberts, R. F.; Allara, D. L.; Pryde, C. A.; Buchanan, P. N. E.; Hobbins, N. D. *Surf. Interface Anal.* **1980**, *2*, 5.
(21) Briggs, D.; Beamson, G. *Anal. Chem.* **1992**, *64*, 1729.
(22) Pireaux, J. J.; Riga, J.; Caudano, R.; Verbist, J. In *Photon, Electron, and Ion Probes of Polymer Structure and Properties*; ACS Symposium Series 162; Dwight, D. W., Fabish, T. J., Thomas, H. R., Eds.; American Chemical Society: Washington, DC, 1981.
(23) Vollhardt, K. P. C. *Organic Chemistry*; W. H. Freeman, New York, 1987.
(24) Briggs, D. *Org. Mass Spectrom.* **1987**, *22*, 91.
(25) Briggs, D.; Brown, A.; Vickerman, J. C. *Handbook of Static Secondary Ion Mass Spectrometry*; Wiley: Chichester, U.K., 1989.

MA950212U